International Journal on Interactive Design and Manufacturing (IJIDeM)
https://doi.org/10.1007/s12008-025-02371-x

ORIGINAL ARTICLE

Development of a morphological parameter and hemodynamic analysis to assess aneurysm operability

Micol Tantillo[1] · Giuseppe Craparo[2] · Antonino Cirello[1] · Gabriele Costantino[2] · Arezia Di Martino[2] · Tommaso Ingrassia[1] · Giuseppe Vincenzo Marannano[1] · Agostino Igor Mirulla[1] · Giovanni Tringali[2] · Vito Ricotta[1]

Received: 3 March 2025 / Accepted: 2 August 2025

Abstract

Cerebral aneurysm is a complex vascular pathology, and the assessment of its rupture risk is often based on qualitative criteria and clinical expertise. The present study aims to develop an objective parameter to support risk evaluation by integrating morphological and hemodynamic analyses. A novel morphological parameter has been introduced, combining key geometric features extracted from 3D vessel reconstructions of middle cerebral artery bifurcations. Computational fluid dynamics (CFD) simulations were conducted to analyze hemodynamic factors such as wall shear stress and intra-aneurysmal pressure, both of which are associated with aneurysm growth and rupture risk. Particular attention was given to defining physiologically accurate boundary conditions, essential for obtaining reliable results. The new morphological parameter alignment with clinical evaluations suggesting its potential to enhance the assessment of aneurysm operability and improve surgical decision-making. This study highlights the importance of integrating morphological and hemodynamic data into the risk assessment process to refine risk stratification and guide more effective treatment strategies.

Graphical Abstract

Schematic representation of the methodological pipeline used to derive a morphological parameter and perform hemodynamic simulations to support surgical decision-making in aneurysm cases

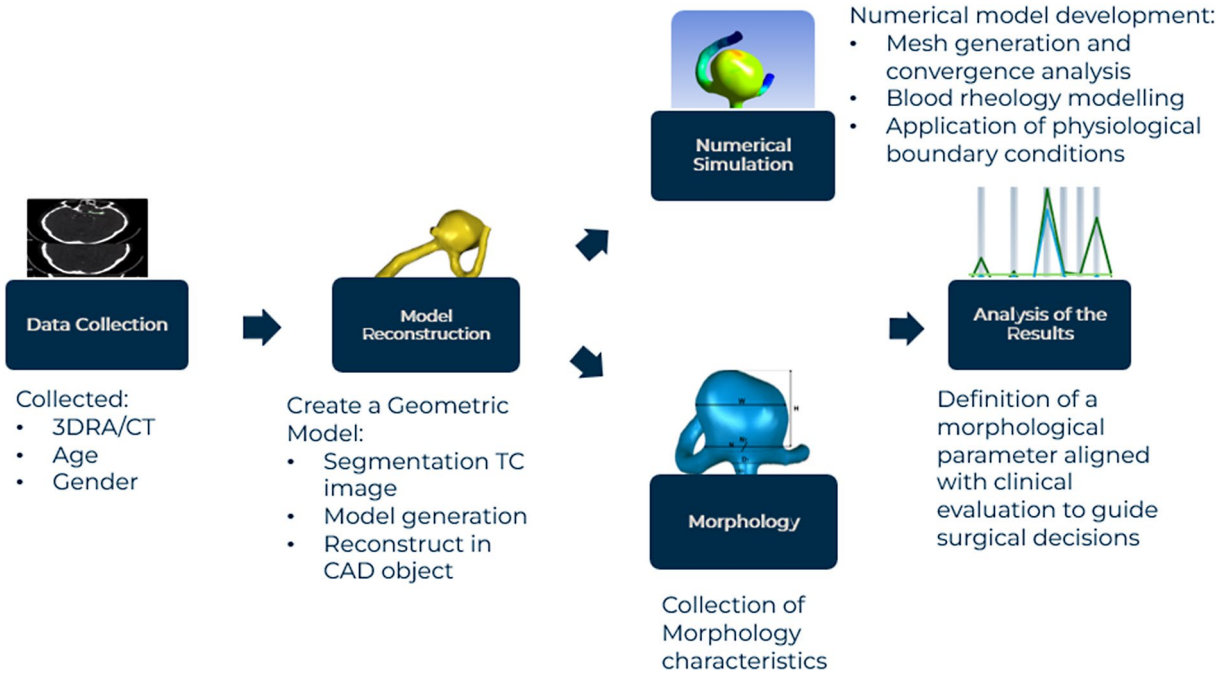

Keywords Cerebral aneurysm · CFD · Morphology · Hemodynamics

Extended author information available on the last page of the article

Published online: 18 August 2025

1 Introduction

Cerebral aneurysms represent abnormal dilations of cerebral arteries, generally caused by a structural deficiency in the arterial wall. Assessing their rupture risk is an important clinical challenge, made more crucial with the increasing diagnostic identification of unruptured aneurysms due to advancement in imaging. The decision between early surgical intervention or conservative monitoring necessitates of precise identification of characteristics that may influence the rupture risk [1–3]. Accurately predicting aneurysm growth and identifying those at higher risk are essential steps in enabling timely and targeted interventions. However, the mechanisms leading to cerebral aneurysm rupture remain poorly understood. Hemodynamic factors are commonly considered pivotal in the pathogenesis, progression, and rupture of aneurysms. By modelling the mechanical forces within the cerebral vessels, Computational Fluid Dynamics (CFD) simulations can help bridge the gap [4–6]. These simulations allow for assessment of hemodynamic stresses implicated in wall degradation and thinning, which may set the stage for aneurysm rupture. However, the application of CFD in clinical practice is limited by the lack of standardized boundary conditions and the absence of robust data that reflect true in vivo conditions. Using 3D anatomical models, CFD enables detailed analysis of blood flow dynamics, including the evaluation of key parameters such as pressure, flow velocity, and wall shear stress (WSS). These simulations allow identifying regions of low wall stress that might correlate with a higher risk of rupture. While studies have shown promising results, the lack of consensus on reliable hemodynamic indicators of rupture risk and the variability in modelling approaches underscore the need for further investigations [7, 8]. Integrating clinical, morphological, and hemodynamic data derived from CFD could provide new insights into the mechanisms driving aneurysm progression and rupture, aiding in the development of more effective and personalized treatment strategies. A key challenge in simulating blood flow within aneurysms is the accurate definition of boundary conditions. Analyzing the velocity profile and flow regime at the inlet is essential to minimize the risk of introducing non-physical effects that could compromise the simulation's accuracy. This step is essential for accurately describing hemodynamic behavior.

This study aimed to evaluate the potential correlation between morphological and hemodynamic characteristics and the risk of cerebral aneurysm rupture. To achieve this, geometries of middle cerebral artery bifurcations were analyzed. Blood flow simulations were conducted under physiological flow conditions, with a detailed examination of the inlet velocity profile. This work seeks to provide a comprehensive characterization of blood flow within aneurysms, with the goal of identifying parameters that improve understanding of the mechanisms underlying aneurysmal rupture.

2 Materials and methods

This study investigates the morphological characteristics and blood flow parameters in middle cerebral artery aneurysms using 3D models reconstructed from medical images. A new parameter has been proposed to characterise aneurysms and facilitate clinical evaluation.

CFD simulations have been performed by imposing boundary conditions that simulate realistic flow and blood rheology settings by focusing on wall shear stress (WSS) and pressure.

The workflow consists of the following phases:

- Geometric model.
- Numerical model.
- Mesh generation and analysis.
- Rheology and blood flow.
- Physiological boundary conditions in CFD simulation.

2.1 Geometric model

The present study is concerned with the characterization of the aneurysm morphology, with a particular focus on those located in the bifurcation of the middle cerebral artery (MCA). To this purpose, data from digital rotational subtraction angiography (3DRA), CT angiography and open datasets have been collected for sixty patients with unruptured MCA aneurysms [9]. The objective was to characterize the size and shape of aneurysms using a morphological parameter. To achieve this, the following information has been collected for each patient: age, gender, and shape parameters.

The vascular geometry has been extracted by importing imaging data into the 3DSlicer segmentation software. A semi-automatic threshold-based procedure was employed to identify the region of interest by differentiating vascular structures from surrounding tissues. To obtain accurate models of blood vessels and aneurysms, this initial segmentation was then refined through manual operations such as cropping and smoothing. This process involved the manual cropping and thresholding of images to distinguish vessels from surrounding tissues. To prepare the models for further analysis, the vessel has been trimmed perpendicular to the axis and extended to approximately seven times the vessel diameter for the MCA inlet and five times for the outflow. This was achieved generative algorithm [10] designed to compute cross-sectional planes orthogonal to generate extensions, ensuring a fully developed flow profile (Fig. 1).

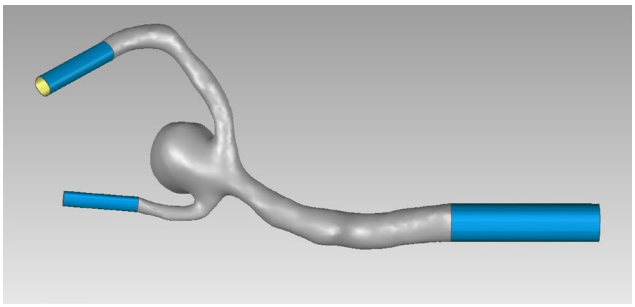

Fig. 1 Example of a reconstructed MCA aneurysm with inlet and outlet extensions for CFD analysis

The workflow was comprised of the following steps:

1. data acquisition.
2. data import into segmentation software.
3. segmentation of vascular structures.
4. exclusion of minor vessels; outlet trimming and extension.
5. export of the obtained vessel geometries as stereolithography (STL) files.

In cases where only 3D models of the vascular structure were available, phase (4) was initiated directly. Shape and dimensions of the aneurysm were evaluated by including the volume of the aneurysm dome, the maximum longitudinal diameter and maximum height of the dome, and the dimensions of the neck, measured in terms of both longitudinal and transverse widths. Moreover, the diameter of the parent vessel (Dv) was determined at a point situated 1.5 times the diameter of the vessel from the bifurcation (D1). The definitions and methodologies for these morphological parameters were derived from established guidelines [2] and are represented in Fig. 2 (A) and 2 (B). The maximum width (W) and height (H) were also measured. The height was defined as the longest dimension from the neck to the tip of the dome, while the width was defined as the maximum longitudinal width. The parameters of the neck were determined as the maximum longitudinal (N) and transverse (NT) widths (Table 1).

Table 1 Summary of patient information and aneurysm measurements, including mean, standard deviation, maximum and minimum values

Aneurysm	Gender		Age (years)	Measurement (mm)	
60	Female	45	57 ± 11 (37–89) years	Height dome	5.60 ± 3.32 (1.31–18.84)
				Width dome	5.01 ± 2.62 (1.14–10.74)
	Male	15		Neck longitudinal width	4.83 ± 2.09 (1.63–10.50)
				Neck width transverse	3.59 ± 1.3 (1.41–8.06)

In addition to these measurements, several dimensionless ratios have also been calculated, such as the height-to-width ratio (H/W), the width-to-neck ratio (W/N), and the height-to-neck ratio (H/N, also known as the aspect ratio), which typically describes the general configuration by providing information about an aneurysm in terms of whether it is elongated or spherical and how it expands in relation to its neck. The study also proposed a new morphological parameter (MP) that combines several key parameters into a single formula. This new parameter has been designed to be easily calculated using two-dimensional data from tomographic or angiographic images and could potentially be used in daily clinical practice. The defined MP is presented in Eq. 1:

$$MP = \frac{W}{N} * \frac{W+N}{2} * H * N_T \tag{1}$$

The development of the MP has been formulated based on clinical indications, which underline the importance of maximum size, symmetry, and shape generally. Each shape parameter included in the MP evaluation was preliminarily

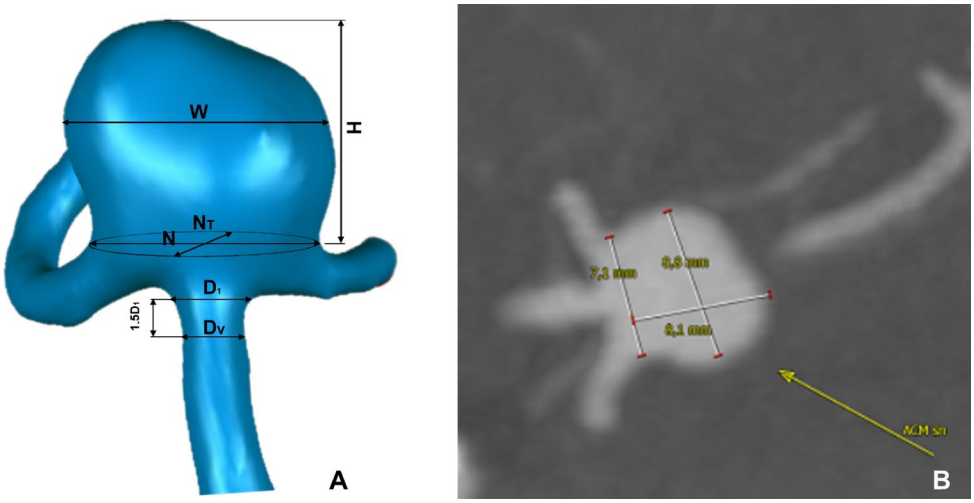

Fig. 2 Visual representation of the methodology used to measure the dimensional parameters of each aneurysm: definitions of the morphological parameters (**A**); aneurysm measurement in the medical image (**B**)

analysed individually in relation to the studied cases, with no evident correlations identified.

2.2 Numerical model

To analyze the flow dynamics within the aneurysm, CFD simulations have been conducted using ANSYS CFX software [11]. After importing the vascular geometries into the solver, the boundary conditions have been carefully defined. A velocity profile has been applied at the inlet. At the same time, an entrainment outflow boundary condition was set at the outlets to limit the influence of the imposed boundary conditions on the mass flow rate partition through the outlets.

The vessel walls have been assumed to be rigid, and no-slip boundary conditions were applied to them. Blood has been treated as an incompressible, non-Newtonian fluid with a density of 1055 kg/m³, ensuring a realistic representation of hemodynamic behavior within the aneurysm.

2.3 Mesh generation and analysis

To ensure accurate resolution of hemodynamic variables, unstructured tetrahedral meshes have been generated, incorporating layers of prismatic cells near the vessel walls to better capture boundary layer effects (Fig. 3). Three different grids have been realized: a fine grid with about 1,400,000 elements, a mid-grid with about 750,000 elements and a coarse mesh with about 350,000 elements, as convergence parameter the average WSS in the dome area has been chosen. A Grid convergence index criteria has been adopted for assessing the required mesh refinement. Even if the best results in terms of GCI, have been obtained with the fine mesh, the mid grid has been chosen for its good computational efficiency and accuracy of the results having a CGI of less than 2% [12].

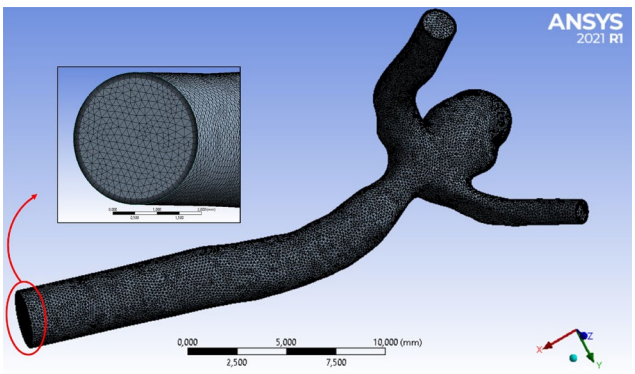

Fig. 3 The mesh is used for simulation, with a close-up view of the inlet region to highlight the prismatic boundary layer

2.4 Rheology and blood flow

The choice between a laminar or turbulent flow model for simulating blood flow aneurysms remains an open question [13–16]. This decision is influenced by factors such as the Reynolds number, the pulsatile nature of blood flow, and the complex geometry of aneurysms [17]. Previous studies have typically assumed laminar flow in intracranial aneurysms, given that the Reynolds number in these cases is typically lower than the threshold for the transition to turbulence in flow through a pipe [16]. However, other studies involving direct numerical simulations (DNS) have confirmed the presence of turbulence in the MCA aneurysms [13].

Turbulence can significantly impact the magnitude of the WSS, which seems a key factor in aneurysm growth and rupture. Often, research on this topic present conflicting results regarding the significance of turbulent versus laminar flow models. For example, in abdominal aortic aneurysms, turbulent models tend to overestimate the mean WSS over time, whereas for intracranial aneurysms, no significant differences have been observed between laminar and turbulent flow models [14]. The choice between a turbulent or laminar flow model depends on the specific application and requires careful consideration of the influencing factors. For some scenarios, laminar flow assumptions are sufficient.

In the present paper, no significant differences have been found between laminar and turbulent flow models for intracranial aneurysms, consistent with previous findings. These results support the idea that both assumptions could be appropriate for simulating the hemodynamic in this context. In addition to flow regime considerations, blood rheology plays a pivotal role in accurately modelling hemodynamic. Blood exhibits non-Newtonian behaviour, with viscosity that decreases as shear rate increases. This shear-thinning behaviour can significantly affect flow characteristics, particularly in regions of low shear stress. For this reason, we employed the Carreau model, which has been shown to effectively describe blood rheology in intracranial aneurysms [18–20].

The Carreau model describes the viscosity of blood as varying with the shear rate and as a function of the time constant (λ), equal to 3.313, the power law index (n), 0.3568, zero shear viscosity (μ_0), equal to 0.056, and the viscosity at infinite shear rate (μ_∞), equal to 0.00345.

In formulating Carreau's model, blood's viscosity is described as follows:

$$\mu = \mu_{\infty} + (\mu_0 - \mu_{\infty})[1 + (\lambda\dot{\gamma})^2]^{\frac{n-1}{2}} \quad (2)$$

2.5 Physiological boundary conditions for CFD simulation

One of the key aspects of this study has been to accurately define the boundary conditions for the simulations to closely replicate the behaviour of blood flow under physiological conditions. The MCA carries approximately 19–21% of the total blood flow in the Circle of Willis, making it a key artery in the cerebral circulation [21]. To define the boundary conditions for the simulations, flow rate data specific to the MCA have been used to calculate both the average and peak velocities at the inlet. A parabolic velocity profile has been applied at the inlet, with an average velocity calculated within the range of 0.4–0.8 m/s based on the mean flow rate of the MCA [21]. This choice ensured that the simulated inflow conditions reflected actual physiological measurements. To gain further insight, we extracted representative velocity profiles of blood flow in the MCA from transcranial Doppler ultrasound data collected from healthy individuals [22]. These profiles provided a precise representation of how blood typically moves through the artery and formed the basis of our boundary condition calculations.

A preliminary CFD analysis was conducted on a straight cylindrical tube, chosen to replicate the conditions within the artery. The tube length was set to 50 times its diameter to ensure sufficient distance for flow stabilisation. Velocity measurements were taken at a location far from the outlet and the inlet to minimise the influence of boundary effects. The resulting profile exhibited a flattened parabola, a consequence of blood's non-Newtonian properties. This observation is consistent with expected flow behaviours for shear-thinning fluids like blood. Using this method, the radial flow profile within the MCA was characterised and used as the basis for defining inlet conditions. In this study, steady-state simulations, were conducted using the flow rate conditions. This assumption is in line with previous studies that have shown the validity of steady-state approaches in aneurysm hemodynamic [23, 24]. At the same time, steady-state simulations allowed us to process a larger dataset, balancing accuracy, and efficiency. A set of CFD analyses has been conducted using an ad hoc developed Fluid Structure Interaction algorithm [25], considering $E = 1.8$ MPa and $\nu = 0.45$ as isotropic material elastic properties [20], finding no significant differences in terms of WSS and maximum pressure within the dome, compared to the fluid dynamic analyses results so this condition has been adopted.

3 Results and discussion

Fluid dynamics provides valuable insights into the pathogenic mechanisms that lead to aneurysm rupture. By analysing blood flow behaviour, it becomes possible to identify factors that contribute to vessel wall weakening and rupture. For each patient, both the hemodynamic conditions and the morphological characteristics influencing the aneurysm were evaluated. In terms of morphology, a novel parameter was developed to establish a threshold capable of distinguishing aneurysms that require surgical intervention. From a hemodynamic perspective, intra-aneurysm pressure (IAP) and WSS have been identified as key indicators for predicting aneurysm progression and rupture [3, 4, 16, 26–28]. WSS, which quantifies the tangential force exerted by blood flow on the vessel wall, is particularly critical for understanding how aneurysms develop structural damage and evolve.

The operability of each aneurysm was assessed by clinicians based on their professional expertise, incorporating qualitative evaluations into the overall analysis. The surgical recommendations were primarily influenced by the aneurysm's shape, including the presence of irregularities, and its maximum size, with aneurysms exceeding 5–7 mm typically classified as severe. This evaluation was further informed by structured interviews with three specialists in the field, who reviewed segmented images to analyse key parameters such as shape and irregularity. This clinical evaluation was integrated into the broader framework to provide a real-world perspective on aneurysm management.

To enhance the understanding of aneurysm operability, a detailed morphological analysis was conducted to identify the geometric parameters most associated with clinical decision-making. Current qualitative tools, such as the PHASES score [29], are widely used in clinical practice to estimate rupture risk but often rely heavily on maximum size as the primary determinant. This approach has been shown to overlook other critical geometric factors, such as shape, volume, and symmetry, which may significantly influence both the risk of rupture and then the need for surgical intervention.

To address this limitation, the new MP integrates maximum size with the aneurysm's overall volumetric shape, offering a more comprehensive assessment of aneurysm geometry. The parameter enables the establishment of a threshold value that helps identify cases where immediate surgical intervention may not be necessary.

The threshold was defined based on the distribution of the morphological parameter across the analyzed cases. As shown in Fig. 3, aneurysms above this value were considered operable by clinicians. The value was empirically determined to reflect actual surgical decisions. This

threshold provides a clear reference point that aligns closely with expert clinical judgment.

Given the absence of universally accepted objective criteria for assessing aneurysm operability, clinical opinion continues to serve as the gold standard. The integration of the MP into the clinical workflow has the potential to ensure that assessments are supported by quantitative morphological data while remaining grounded in the expertise of experienced clinicians. This combined approach leverages numerical insights to validate and enhance professional judgment.

The results reveal a good alignment between the MP and expert clinical evaluations, emphasizing its potential as a reliable and practical tool for assessing aneurysm risk.

Among the sixty aneurysms evaluated, thirty-eight were deemed to be operable based on clinical judgment. The PHASES score correctly identified 53% of these cases, whereas the Morphology Parameter demonstrated a significantly higher accuracy, correctly identifying 89% of operable aneurysms. The operability indicator is indicated in the graph (Fig. 4) by grey bars, while the MP and PHASES score values are represented by green and blue markers, respectively. This comparison underscores the effectiveness of the MP in identifying high-risk aneurysms, offering a more precise tool for clinical decision-making.

The multidimensional nature of the MP enables it to capture aspects of the aneurysm's overall structure, demonstrating a good concordance with clinical evaluations. For example, even smaller aneurysms may exhibit structural characteristics, such as a wide neck or irregular shape, which elevate their risk of rupture. This highlights the limitations of relying solely on maximum size-based metrics. Furthermore, rupture risk is influenced by more than just aneurysm size.

As a volumetric measure, the MP may better reflect the mechanical forces contributing to wall degeneration, offering a more comprehensive perspective on aneurysm stability. By accounting for these factors, the MP provides a robust framework for assessing rupture risk and guiding surgical decision-making.

The graph in Fig. 5 illustrates the normalised WSS values for patients, organised by MP increasing aneurysms. The green line represents the average WSS measured at the aneurysm dome while the grey bars indicate whether surgical intervention was performed.

In smaller aneurysms (left side of the graph), WSS values show significant variability, this could be indicative of hemodynamic variability, which may be associated with higher risk of rupture. Conversely, larger aneurysms (right side of the graph) demonstrate consistently lower WSS values. This behaviour corresponds to the low WSS, which is characterised by slower flow and reduced shear stress, as commonly observed in larger aneurysms [7]. The graph thus indicates a decreasing trend in WSS with increasing aneurysm size. These findings are consistent with the observations of Tang et al. [26], who similarly described a transition from high WSS in small aneurysms to low WSS in larger ones. This evidence supports the hypothesis that WSS is a crucial parameter for risk assessment and decision-making in clinical practice, providing a valuable framework for monitoring aneurysm progression and guiding therapeutic interventions. The graph of intra aneurysm pressure (Fig. 6), measured at the aneurysm dome, showed no clear association with medical opinions and the new parameter MP, making predictions unreliable, suggesting that pressure may not

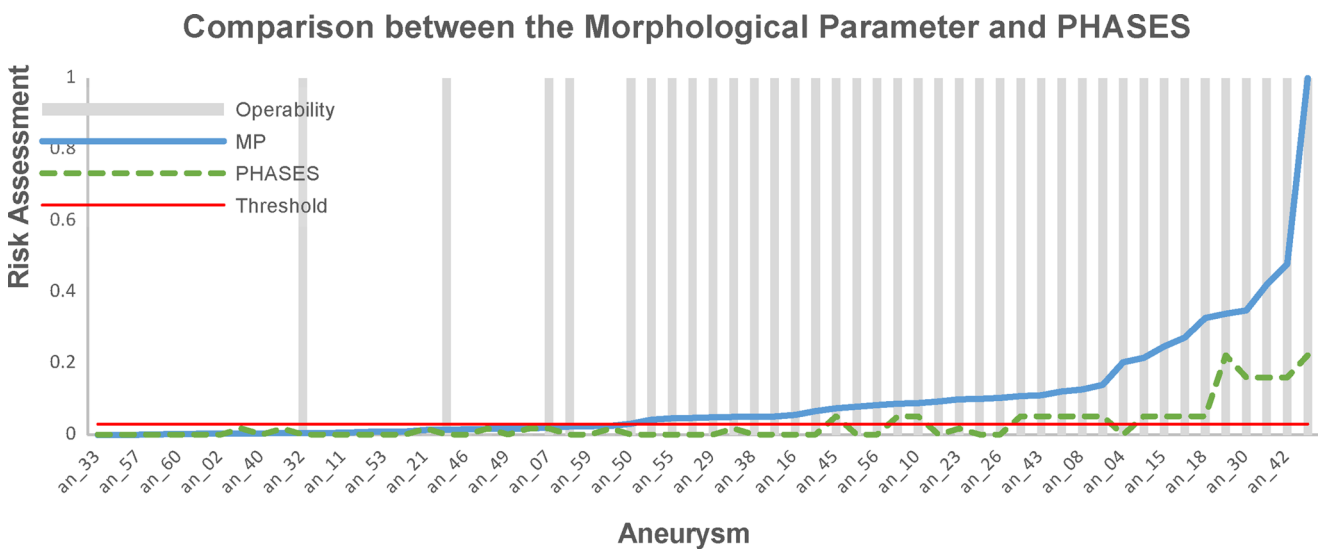

Fig. 4 The graph shows the data for each aneurysm as MP values increase, including the threshold. Includes bars indicating whether the aneurysm is operable and another curve representing the PHASES value. For the y-axis, the risk assessment is displayed (0 = no risk; 1 = high risk)

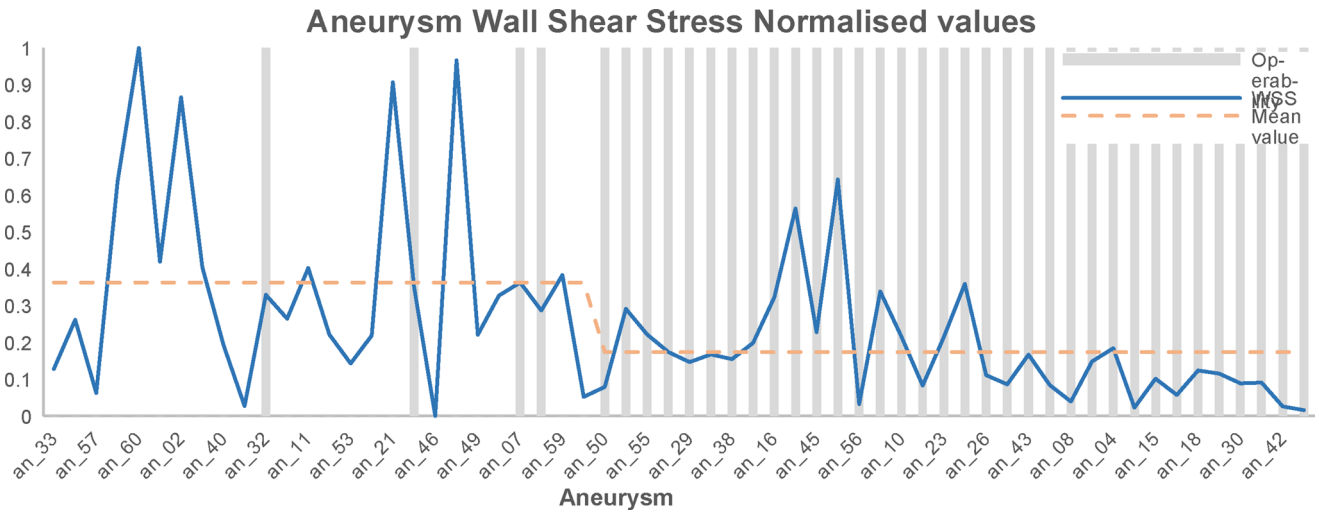

Fig. 5 The graph illustrates WSS values as MP values increase

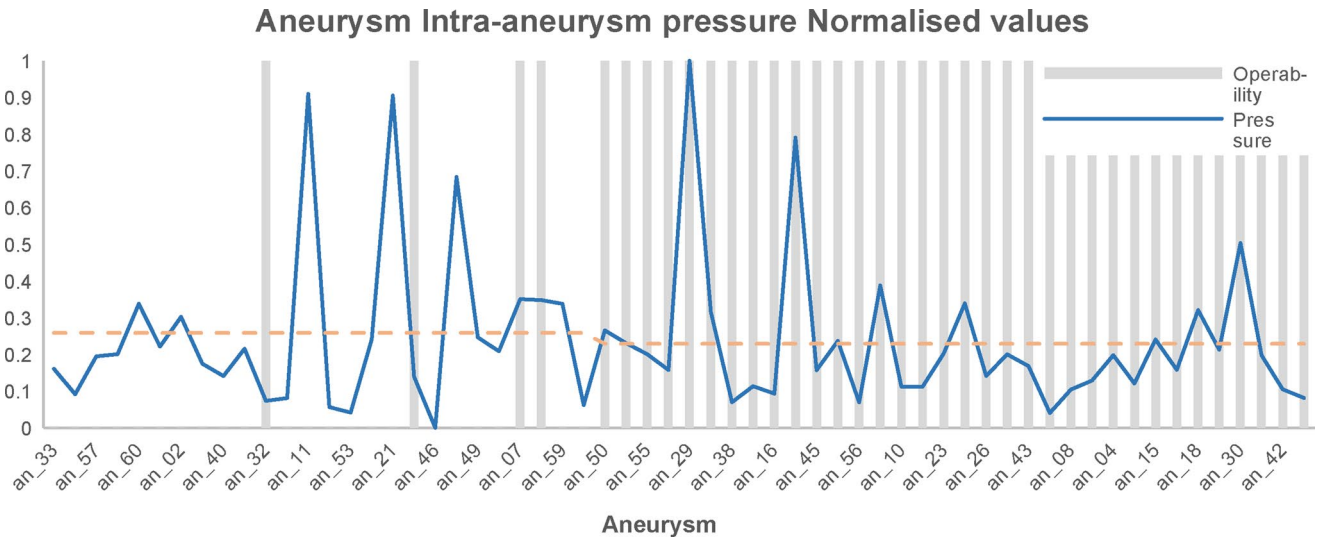

Fig. 6 The graph illustrates aneurysm pressure values as MP values increase

be helpful in assessing rupture risk, but may be more relevant to aneurysm growth. Figure 7 shows an example of wall shear stress and pressure distribution maps on a representative MCA bifurcation aneurysm model. Further studies are needed to understand its role and how it could be used in clinical decisions.

4 Conclusion

The integration of morphological and hemodynamic parameters could allow to achieve a more comprehensive and objective assessment of cerebral aneurysm rupture risk. In this regard, this study valuated novel metrics, such as the proposed MP, using CFD simulations and a detailed morphological characterisation. Capturing the multidimensional nature of aneurysm geometry and providing valuable insight into structural features such as irregular shapes that influence the risk of rupture, the MP parameter could improve the accuracy of risk assessment compared to traditional size-based approaches. Its correlation with expert clinical evaluation highlights its potential as a reliable quantitative tool to complement current qualitative methods.

From a hemodynamic perspective, WSS emerged as a critical factor for evaluating aneurysm stability. Smaller aneurysms exhibited high WSS variability, potentially indicative of growth or rupture risk, whereas larger aneurysms consistently demonstrated low WSS values, supporting a low-flow regime hypothesis. This highlights the importance of a multi-parametric approach to aneurysm analysis given the complex mechanisms underlying rupture. Expanding the dataset would also improve the accuracy

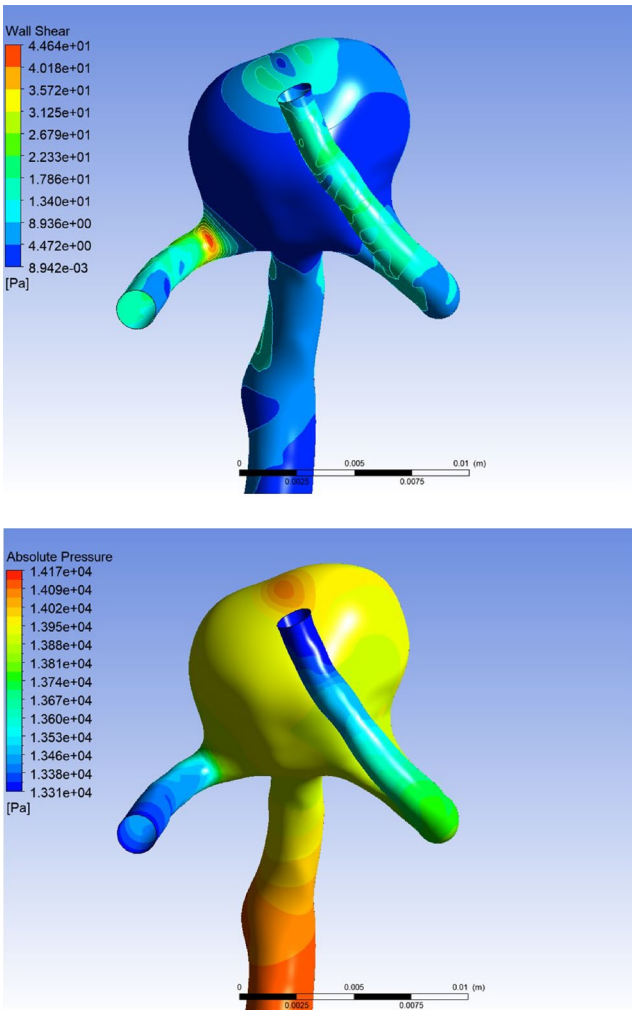

Fig. 7 Wall shear stress distribution (top) and pressure map (bottom) on a representative middle cerebral artery (MCA) bifurcation aneurysm obtained from CFD simulations

of models and broaden their applicability, particularly for small or complex aneurysms. Longitudinal studies could provide a clearer understanding of how aneurysms progress under varying haemodynamic conditions.

Funding Open access funding provided by Università degli Studi di Palermo within the CRUI-CARE Agreement.

Data availability The authors declare that the data supporting the findings of this study are available within the paper.

Declarations

Competing interests The authors declare that they have no known competing financial interests or personal relationships that could have appeared to influence the work reported in this paper.

References

1. Shen, J., Huang, K., Zhu, Y., Weng, Y., Xiao, F., Mungur, R., Wu, F., Pan, J., Zhan, R.: Mean arterial pressure-aneurysm neck ratio predicts the rupture risk of intracranial aneurysm by reflecting pressure at the dome. Front. Aging Neurosci. **15**, 1082800 (2023). https://doi.org/10.3389/fnagi.2023.1082800
2. Dhar, S., Tremmel, M., Mocco, J., Kim, M., Yamamoto, J., Siddiqui, A.H., Hopkins, L.N., Meng, H.: MORPHOLOGY PARAMETERS FOR INTRACRANIAL ANEURYSM RUPTURE RISK ASSESSMENT. Neurosurgery. **63**, 185–197 (2008). https://doi.org/10.1227/01.NEU.0000316847.64140.81
3. Fujimura, S., Yamanaka, Y., Takao, H., Ishibashi, T., Otani, K., Karagiozov, K., Fukudome, K., Yamamoto, M., Murayama, Y.: Hemodynamic and morphological differences in cerebral aneurysms between before and after rupture. J. Neurosurg. **140**, 774–782 (2024). https://doi.org/10.3171/2023.6.JNS23289
4. Saqr, K.M., Rashad, S., Tupin, S., Niizuma, K., Hassan, T., Tominaga, T., Ohta, M.: What does computational fluid dynamics tell Us about intracranial aneurysms? A meta-analysis and critical review. J. Cereb. Blood Flow. Metab. **40**, 1021–1039 (2020). https://doi.org/10.1177/0271678X19854640
5. Cebral, J.R., Mut, F., Weir, J., Putman, C.: Quantitative characterization of the hemodynamic environment in ruptured and unruptured brain aneurysms. AJNR Am. J. Neuroradiol. **32**, 145–151 (2011). https://doi.org/10.3174/ajnr.A2419
6. Schena, M., Testa, F., Bozzetto, M., Remuzzi, A., Lanterna, L.A.A., Lanzarone, E.: A CFD-based framework to evaluate surgical alternatives in cerebral aneurysms. Comput. Methods Biomech. Biomedical Engineering: Imaging Visualization. **12**, 2325351 (2024). https://doi.org/10.1080/21681163.2024.2325351
7. Wei, H., Tian, Q., Yao, K., Wang, J., He, P., Guo, Y., Han, W., Gao, W., Li, M.: Different hemodynamic characteristics and resulting in different risks of rupture between Wide-Neck and Narrow-Neck aneurysms. Front. Neurol. **13**, 868652 (2022). https://doi.org/10.3389/fneur.2022.868652
8. Amigo, N., Valencia, Á.: Determining significant morphological and hemodynamic parameters to assess the rupture risk of cerebral aneurysms. J. Med. Biol. Eng. **39**, 329–335 (2019). https://doi.org/10.1007/s40846-018-0403-0
9. Pozo, J.M., Frangi, A.F.: Database of cerebral artery geometries including aneurysms at the middle cerebral artery bifurcation
10. Cirello, A., Ingrassia, T., Marannano, G., Mirulla, A.I., Nigrelli, V., Petrucci, G., Ricotta, V.: A new automatic process based on generative design for CAD modeling and manufacturing of customized orthosis. Appl. Sci. **14**, 6231 (2024). https://doi.org/10.3390/app14146231
11. Cirello, A., Ingrassia, T., Nigrelli, V.: Study of the performances of a fluidynamic actuator. Int. J. Mech. Eng. Technol. **9**, 859–866 (2018)
12. Roache, P.J.: Verification and validation in computational science and engineering

13. Valen-Sendstad, K., Mardal, K.-A., Mortensen, M., Reif, B.A.P., Langtangen, H.P.: Direct numerical simulation of transitional flow in a patient-specific intracranial aneurysm. J. Biomech. **44**, 2826–2832 (2011). https://doi.org/10.1016/j.jbiomech.2011.08.015
14. Brambila-Solórzano, A., Méndez-Lavielle, F., Naude, J.L., Martínez-Sánchez, G.J., García-Rebolledo, A., Hernández, B.: Escobar-del Pozo, C.: Influence of blood rheology and turbulence models in the numerical simulation of aneurysms. Bio. Eng. **10**, 1170 (2023). https://doi.org/10.3390/bioengineering10101170
15. Luciano, R.D., Da Silva, B.L., Chen, X.B., Bergstrom, D.J.: Turbulent blood flow in a cerebral artery with an aneurysm. J. Biomech. **172**, 112214 (2024). https://doi.org/10.1016/j.jbiomech.2024.112214
16. Korte, J., Klopp, E.S., Berg, P.: Multi-Dimensional modeling of cerebral hemodynamics: A systematic review. Bioengineering. **11**, 72 (2024). https://doi.org/10.3390/bioengineering11010072
17. Asgharzadeh, H., Borazjani, I.: Effects of reynolds and womersley numbers on the hemodynamics of intracranial aneurysms. Comput. Math. Methods Med. 1–16 (2016). https://doi.org/10.1155/2016/7412926
18. Moradicheghamahi, J., Sadeghiseraji, J., Jahangiri, M.: Numerical solution of the pulsatile, non-Newtonian and turbulent blood flow in a patient specific elastic carotid artery. Int. J. Mech. Sci. **150**, 393–403 (2019). https://doi.org/10.1016/j.ijmecsci.2018.10.046
19. Yang, H., Hong, I., Kim, Y.B., Cho, K.-C., Oh, J.H.: Influence of blood viscosity models and boundary conditions on the computation of hemodynamic parameters in cerebral aneurysms using computational fluid dynamics. Acta Neurochir. **165**, 471–482 (2023). https://doi.org/10.1007/s00701-022-05467-5
20. Paz, C., Suárez, E., Cabarcos, A., Pinto, S.I.S.: Numerical study of a thrombus migration risk in aneurysm after coil embolization in patient cases: FSI modelling. Cardiovasc. Eng. Tech. **14**, 544–559 (2023). https://doi.org/10.1007/s13239-023-00672-4
21. Zarrinkoob, L., Ambarki, K., Wåhlin, A., Birgander, R., Eklund, A., Malm, J.: Blood flow distribution in cerebral arteries. J. Cereb. Blood Flow. Metab. **35**, 648–654 (2015). https://doi.org/10.1038/jcbfm.2014.241
22. Wadehn, F., Heldt, T.: Adaptive maximal blood flow velocity Estimation from transcranial doppler echos. IEEE J. Transl Eng. Health Med. **8**, 1–11 (2020). https://doi.org/10.1109/JTEHM.2020.3011562
23. Geers, A.J., Larrabide, I., Morales, H.G., Frangi, A.F.: Approximating hemodynamics of cerebral aneurysms with steady flow simulations. J. Biomech. **47**, 178–185 (2014). https://doi.org/10.1016/j.jbiomech.2013.09.033
24. Schena, M., Testa, F., Bozzetto, M., Remuzzi, A., Lanterna, L.A.A., Lanzarone, E.: A CFD-based framework to evaluate surgical alternatives in cerebral aneurysms. Comput. Methods Biomech. Biomed. Eng. Imaging Vis. **12**, 2325351 (2024). https://doi.org/10.1080/21681163.2024.2325351
25. Cirello, A., Ingrassia, T., Mancuso, A., Nigrelli, V., Tumino, D.: Improving the downwind sail design process by means of a novel FSI approach. JMSE. **9**, 624 (2021). https://doi.org/10.3390/jmse9060624
26. Tang, Y., Wei, H., Zhang, Z., Fu, M., Feng, J., Li, Z., Liu, X., Wu, Y., Zhang, J., You, W., Xue, R., Zhuo, Y., Jiang, Y., Li, Y., Li, R., Liu, P.: Transition of intracranial aneurysmal wall enhancement from high to low wall shear stress mediation with size increase: A hemodynamic study based on 7T magnetic resonance imaging. Heliyon. **10**, e30006 (2024). https://doi.org/10.1016/j.heliyon.2024.e30006
27. Wang, F., Xu, B., Sun, Z., Wu, C., Zhang, X.: Wall shear stress in intracranial aneurysms and adjacent arteries. Neural Regen Res. (2013).
28. Geers, A.J., Morales, H.G., Larrabide, I., Butakoff, C., Bijlenga, P., Frangi, A.F.: Wall shear stress at the initiation site of cerebral aneurysms. Biomech. Model. Mechanobiol. **16**, 97–115 (2017). https://doi.org/10.1007/s10237-016-0804-3
29. Greving, J.P., Wermer, M.J.H., Brown, R.D., Morita, A., Juvela, S., Yonekura, M., Ishibashi, T., Torner, J.C., Nakayama, T., Rinkel, G.J.E., Algra, A.: Development of the PHASES score for prediction of risk of rupture of intracranial aneurysms: A pooled analysis of six prospective cohort studies. Lancet Neurol. **13**, 59–66 (2014). https://doi.org/10.1016/S1474-4422(13)70263-1

Authors and Affiliations

Micol Tantillo[1] · Giuseppe Craparo[2] · Antonino Cirello[1] · Gabriele Costantino[2] · Arezia Di Martino[2] · Tommaso Ingrassia[1] · Giuseppe Vincenzo Marannano[1] · Agostino Igor Mirulla[1] · Giovanni Tringali[2] · Vito Ricotta[1]

✉ Micol Tantillo
micol.tantillo@unipa.it

Giuseppe Craparo
giuseppe.craparo@arnascivico.it

Antonino Cirello
antonino.cirello@unipa.it

Gabriele Costantino
gabriele.costantino@anrnascivico.it

Arezia Di Martino
arezia.dimartino@arnascivico.it

Tommaso Ingrassia
tommaso.ingrassia@unipa.it

Giuseppe Vincenzo Marannano
Giuseppe.marannano@unipa.it

Agostino Igor Mirulla
agostinoigor.mirulla@unipa.it

Giovanni Tringali
giovanni.tringali@arnascivico.it

Vito Ricotta
vito.ricotta@unipa.it

[1] Department of Engineering, University, University of Palermo, Palermo, Italy

[2] Neurosurgery Department University, ARNAS Civico Di Cristina Benfratelli Hospital, Palermo, Italy